Earlier comment on title: "surrogate"

A Study of Two Neutron Transfer Reactions in the Zr Isotopes: DRAFT

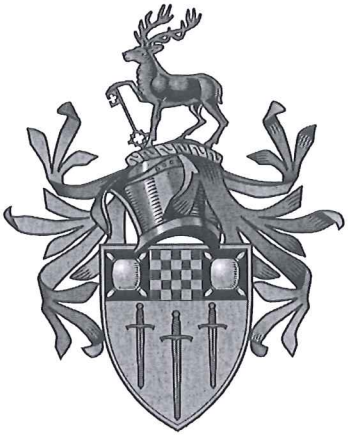

James Benstead

Submitted for the degree of Doctor of Philosophy

~~Under the supervision of J. A. Tostevin~~ → to Acknow!

Department of Physics,

University of Surrey,

Guildford,

GU2 7XH

September 11, 2014

People read this: So should be carefully written

excitation energy,

Abstract

A theoretical model has been developed to predict the spin and parity distributions of the residual nucleus remaining following a (p,t) two neutron transfer reaction. These distributions may be compared against those expected for the same nucleus produced via an (n,γ) reaction and therefore provide information on whether (p,t) can be used as a suitable surrogate in cases where an (n,γ) reaction can not be observed directly. This model predicts the possible J^{π} and energy values of the discrete excited states which may be populated in the residual nucleus and calculates the strength of each transition, including both the kinematic and structural components of the cross section. The model has been designed to be purely predictive and to require little or no prior information regarding the target nucleus in question. The model developed has been applied to the case of 28.53 MeV protons incident on an isotopically enriched ^{92}Zr target, a case for which experimental data have recently been taken using the STARLiTeR detector at Texas A&M University. Data exist for the triton energy spectrum, triton angular distributions in the range $\theta \approx 25°$ - 60°, and coincident γ-ray decay spectra. The preliminary comparison between the model and data shows a reasonable match to the average trends, but a breakdown when individual discrete states are scutinised in detail. In particular, the model fails to predict the existence of a number of states observed in ^{90}Zr, suggesting a more sophisticated approach to the structural calculations included is required.

not prelim for thesis

with residual The developed dynamical detailed on A detailed Population and/or dynamical components of the model physical

Acknowledgements

Contents

List of Figures

List of Tables

Background / exemplar cases referenced here is important.

Chapter 1

Introduction

1.1 Surrogate reaction method

measured?

[references?]

Theoretical

Calculations of neutron induced reaction cross sections rarely produce perfect matches to the true physical values. Often, experimental data are required to constrain the inputs to a calculation, or even to scale the results. The fidelity of calculations generally decreases as one moves further from the *line of stability* on the Chart of the Nuclides, often referred to as a Segré chart [].

the

directly

of interest

induced

Unfortunately, for many isotopes it is not possible to conduct conventional neutron cross section measurements. There are various reasons why it may not be possible to measure a certain nuclear reaction directly. Most common amongst these reasons is too short a lifetime for the target nucleus in question. This is especially relevant for many of the isotopes produced during fission, which are generally neutron-rich and rapidly undergo β-decay. [references]

The majority of reactions of interest to the nuclear industry, and many relevant to astrophysics, involve the collision of an incident neutron with a target nucleus. Aside from elastic scattering, the reactions which may occur due to an incident neutron typically take place through an intermediate compound nucleus state, as shown in figure 1.2.

to produce a target for the

Important examples?

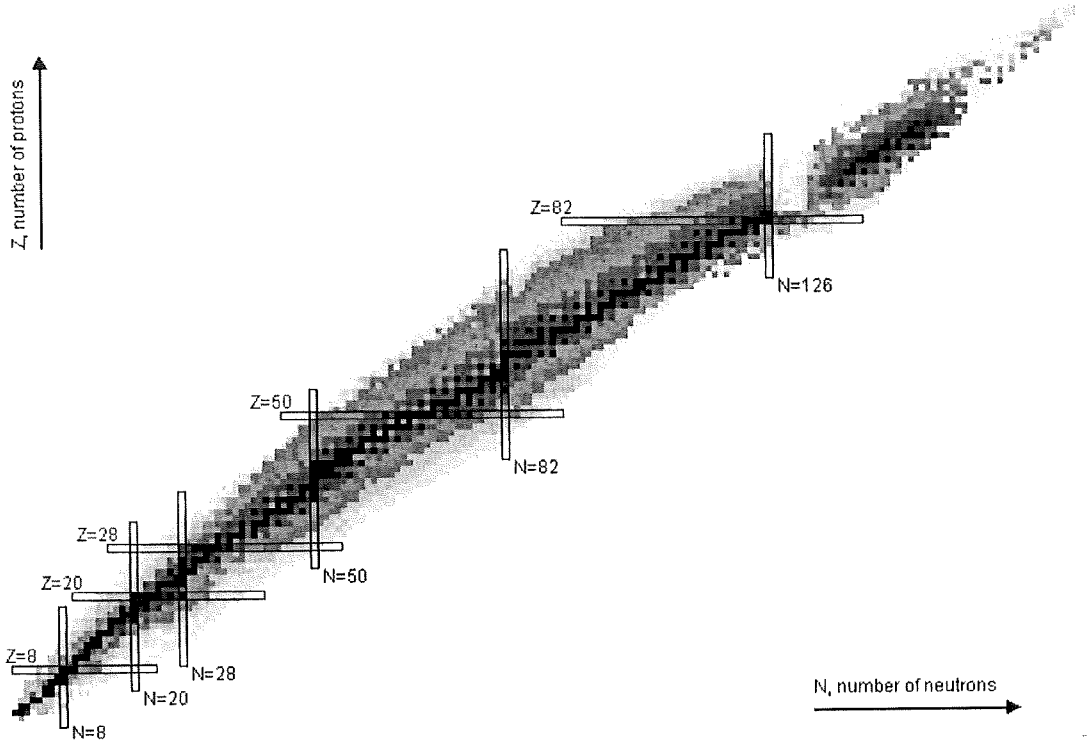

Figure 1.1: The Chart of the Nuclides, showing the line of nuclear stability in black. Created using [].

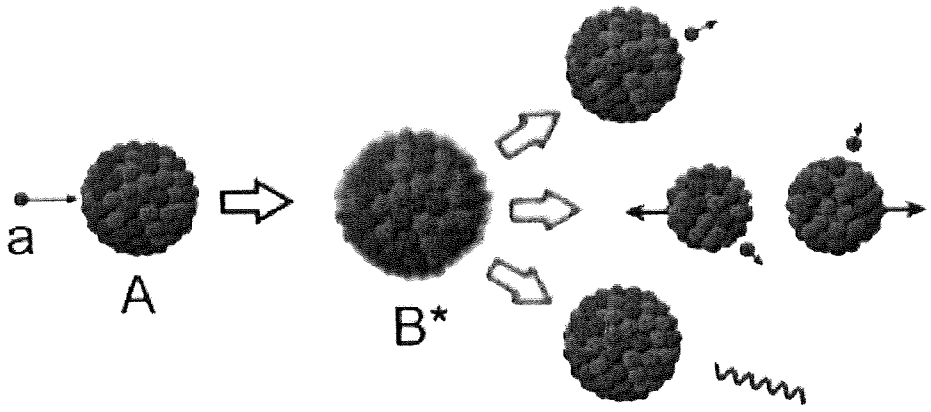

Figure 1.2: Illustration of a nuclear reaction proceeding through the compound nucleus stage. a collides with A to form B^*, which then decays to a number of possible products.

Here the incident neutron is absorbed by the target nucleus and forms an excited compound nucleus. This compound nucleus is unstable and will decay after some time to form the final products of the reaction. The surrogate reaction method exploits the Bohr assumption, that the mode of decay of a compound nucleus is independent of the type of reaction from which it formed []. It is assumed that only the *spin distribution* of the states, in both energy and angular momentum, populated in the compound nucleus plays a role in determining the statistical likelihood of decays via each possible channel.

In the surrogate reaction method, a suitable *surrogate* nucleus and reaction are sought, such that the same compound nucleus spin distribution will be formed as would be expected in the reaction of interest. The surrogate process is illustrated in figure 1.3.

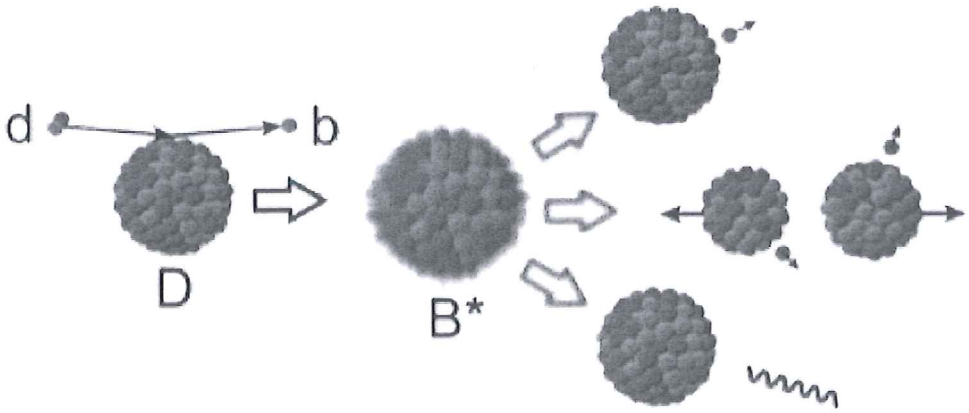

Figure 1.3: Illustration of the surrogate reaction method. Here, d interacts with D to form the compound nucleus B^*, which then decays in the same manner as would be expected through the desired reaction. d may simply be scattered inelastically, but most often loses or gains nucleons to form particle b.

In the surrogate method, one wishes to determine the cross section $\sigma_{\alpha\chi}(E_a)$ for a reaction with incident channel α $(a+A)$ at an incident energy E_a and exit channel χ. $\sigma_{\alpha\chi}(E_a)$ may be broken into two components, as shown in equation (1.1)

$$\sigma_{\alpha\chi}(E_a) = \sum_{J,\pi} \sigma_\alpha^{\mathrm{CN}}(E_{\mathrm{ex}}, J, \pi)\, G_\chi^{\mathrm{CN}}(E_{\mathrm{ex}}, J, \pi) \ . \tag{1.1}$$

Here $\sigma_\alpha^{\mathrm{CN}}(E_{\mathrm{ex}}, J, \pi)$ is the cross section for forming the compound nucleus B^* in the desired reaction channel and $G_\chi^{\mathrm{CN}}(E_{\mathrm{ex}}, J, \pi)$ is the probability of B^* decaying via channel χ.

In a standard measurement both $\sigma_\alpha^{\mathrm{CN}}(E_{\mathrm{ex}}, J, \pi)$ and $G_\chi^{\mathrm{CN}}(E_{\mathrm{ex}}, J, \pi)$ are measured directly. In the surrogate approach however, only $G_\chi^{\mathrm{CN}}(E_{\mathrm{ex}}, J, \pi)$ is measured and $\sigma_\alpha^{\mathrm{CN}}(E_{\mathrm{ex}}, J, \pi)$ is instead calculated. The surrogate approach is therefore a hybrid of theory and experiment. There are obviously greater subtleties to the method than a single equation and figure, however the description given above serves to convey the basics.

The surrogate method was first applied in the 1970s to the (n,f) reaction by e.g. Cramer and Britt [] and then Britt and Wilhelmy []. These studies employed the Weisskopf-Ewing approximation [], which assumes that the probability of decay via any channel is independent of the J^π components of the compound nucleus spin distribution, i.e. it is only dependent upon the excitation energy $G_\chi^{\mathrm{CN}}(E_{\mathrm{ex}}, J, \pi) \rightarrow G_\chi^{\mathrm{CN}}(E_{\mathrm{ex}})$. These early surrogate studies showed a good match against available direct measurements of the desired reaction, above energies of $\approx$1 MeV, to an accuracy of 10 - 20%. A match to the data ~~of less than~~ 20% would generally be considered better than that expected from a purely theoretical calculation [].

Interest in the surrogate method has been rekindled in the last decade, with dedicated surrogate groups forming in both the US and France, and with smaller scale efforts also underway in India and Japan. These groups have largely focussed their efforts upon measurements of the (n,f) cross sections of minor actinides in support of nuclear fuel cycle applications []. An excellent 2012 paper by Escher et al. [] gives detailed descriptions of both the surrogate method and the current worldwide experimental programmes. The results of modern (n,f) surrogate measurements compare favourably with direct experimental data. However, generally, for each isotope studied, this match breaks down at lower excitation energies and also, in

some cases, above the threshold for second chance fission [].

The poorer performance of the surrogate method in certain energy regions is due to a so-called *spin mismatch* and the breakdown of the validity of the Weisskopf-Ewing approximation. At low excitation energies the possible levels which a nucleus may occupy are discretely spaced out in energy, with each level possessing a unique J^π assignment. As excitation energy increases, the density of levels increases until eventually a continuum of states is reached. At lower excitation energies, a very particular spin distribution must be imparted to a target nucleus in order to occupy the levels available with the same distribution strength as in the desired reaction channel. A surrogate reaction may therefore quite easily populate a different spin distribution in this lower energy region if the reaction used tends to transfer very different values of J^π.

For fissile nuclei at higher excitation energies, the (n,f) channel is generally dominant and the distribution of fragments generated, which may be altered by the differing fission decay channels taken, is not important, but rather, it is the integrated (n,f) cross section to all final products which is the value of concern. In other words, although the decay path taken from a higher excitation energy state may be different in the surrogate case compared to that of the desired reaction, it will still result in the production of fission fragments and hence the same (n,f) cross section.

The limitations of the surrogate method, due to spin-mismatch, are greater for the case of the (n,γ) reaction. The (n,γ) reaction is of importance to both nuclear industry and to an understanding of key astrophysical processes, such as the stellar $s-$ and $r-$processes []. Surrogate (n,γ) studies, e.g. by Scielzo et al [], have shown that for the current surrogate approaches employed, a more sophisticated application of theory is required to take into account the differences in spin-distribution between the desired and surrogate cases.

In parallel to efforts to develop additional theory to 'translate' from a measured spin distribution to the expected one, it is worth exploring new types of surrogate reactions which may populate spin distributions closer to that expected in the desired reaction. Although early studies employed the (t,p) reaction as a surrogate, no

Anything general to be said about nature of states populated. (p,t) removes 2n so populates hole like configs. IS this bad? (n,g) populates particle like?

studies have been reported which utilise the (p,t) transfer reaction.

In this study we have therefore developed a model for performing (p,t) calculations over a range of excitation energies, in order to predict the observables of a typical surrogate measurement. This model has been designed to require only very limited prior information regarding the target nucleus to which it is applied, with the hope that it can be taken and applied relatively quickly to a range of isotopes in order to better inform the selection of candidate surrogate experiments, i.e. those in which the spin-mismatch is likely to be at a minimum. This developed model has been applied to a recent measurement of the ^{92}Zr(p,t)^{90}Zr reaction.

1.2 (p,t) transfer reactions

Nuclear reactions may be divided into three broad categories; compound nucleus, pre-equilibrium and direct. Reactions may be placed into these categories based upon their timescales and also the number of collisions which occur between the constituent nucleons of the target and the incident nuclei [].

Compound nucleus reactions occur over the longest timescales ($\approx 10^{-15}$s) and involve a large number of collisions and sharing of energy between the incident particle and the nucleons present within the target nucleus. Direct reactions occur over the shortest timescales ($\approx 10^{-21}$s) and typically involve collisions between the incident particle and only one or two of the nucleons of the target nucleus. Pre-equilibrium reactions occupy the middle ground between these two reaction types in terms of timescale and number of collisions.

At relatively low energies (of a few MeV per nucleon) direct reactions are more likely to occur for charged incident particles, as the Coulomb potential between the nuclei will hinder their ability to appreciably penetrate beyond the surface and form a compound nucleus. For a significant fraction of direct reactions to occur, the energy of the incident charged particle must also be higher than the Coulomb barrier of the target nucleus, otherwise it will be deflected via Rutherford scattering before a short-distance collision can take place.

Transfer reactions, a category of direct reactions, involve the transfer of a nucleon, or a cluster of nucleons, either to or from a projectile when incident on a target nucleus. When the projectile removes a nucleon from the target, e.g. in a (p,d) reaction, it is referred to as *pickup*. When the projectile loses a nucleon, e.g. in the (d,p) reaction, it is referred to as *stripping*.

The (p,t) reaction was first studied in the 1950s, where a simple Plane Wave Born Approximation approach (see section 2.3.1) was applied to single step transfers of di-neutron clusters by e.g. El Nadi [?, ?]. The more sophisticated Distorted Wave Born Approximation (DWBA) (see section 2.3.2) was applied next, which took into account competing elastic and compound nucleus reaction channels. Methods were developed by Moshinsky [], and later extended by Bayman and Kallio [], to translate the properties of two individual neutrons into the properties of a single di-neutron cluster and to calculate the probability amplitudes for such a configuration.

These early calculations assumed a zero range approximation to the triton wavefunction which forbids the population of so-called unnatural parity states in the reaction when an even-even nucleus is considered as the target (see section 2.4). 'Forbidden' transitions were however observed in (p,t) reactions on a number of isotopes, e.g. ^{208}Pb(p,t)$^{206}_{3^+}$ []. Methods for incorporating two step processes into (p,t) DWBA calculations were developed by e.g. Asciutto and Glendenning [?, ?], which allowed these previously forbidden transitions to occur. Two step processes were also found to be required to explain the cross sections and angular distributions measured for a number of natural parity transitions which had previously only been considered using standard one step DWBA calculations, e.g. the ^{116}Sn(p,t)Sn$^{114}_{0^+_{gs}}$ reaction [].

A number of authors, including e.g. Nagarajan et al [], found that a number of these forbidden transitions or discrepent datasets could instead be explained by introducing a more realistic finite range triton wave function into calculations. This more realistic wavefunction included a small higher angular momentum component, which allows for the population of unnatural parity states [].

Methods beyond the DWBA approach, such as coupled channels calculations

have been applied extensively to (p,t), by e.g Thompson []. These calculations are able to demonstrate the contributions and importance of competing reaction pathways. In general however, the standard one step DWBA approach using a zero range approximation is considered appropriate for use with most spherical target nuclei, with higher order processes only considered as standard for deformed nuclei with strong coupling to collective modes of excitation []. This standard one step di-neutron DWBA approach will also be applied in this study and higher order processes only considered if forbidden states are observed in the experimental data or there are large discrepencies when attempting to match the measured data for allowed transitions.

(p,t) measurements have previously been performed for the Zr isotopes by Ball et al [?, ?] with detailed comparisons against theoretical calculations also made. Given a desire to create a generic (p,t) model which can be applied to any target nucleus, regardless of prior data being available or not, we have not used this prior study to influence the model's development. However, we do compare our calculated results against these early Zr (p,t) data (see section 5.6.2). Furthermore, we are infact influenced by this previous work in that their assessment is that for (p,t) reactions on Zr, higher order processes are not required and a simple one step DWBA approach is sufficient.

The main body of this work is divided into the following chapters. Chapter 2 describes calculations of two neutron transfer reactions, including both the kinematic DWBA component and necessary structural factors. Chapter 3 describes the specifics of performing these calculations for the Zr isotopes as well as the methods for determining the energy spectrum of the states excited in ^{90}Zr. Chapter 4 outlines the experimental setup and how the theoretical results should be presented in order to allow for comparison with the measured data. Chapter 5 reports the results of this study and the comparison against the experimental data. Chapter 6 outlines potential methods for enhancing or extending the developed model and finally chapter 7 provides a summary of the work performed, draws conclusions and identifies potential areas of future study.

Many body system. Empirically, clusters of single particle energies separated by gaps at magic #'s, 2, 8, 20, 50, 82, 126. Consistent with nucleons seeing, predominantly, a central mean field potential plus a strong attractive spin-orbit potential. Basis of shell-model picture of nuclear single-particle behavior. [refs to texts].

Chapter 2

Two Neutron Transfer Reactions

In this chapter we develop and describe the necessary formalisms for calculating the physical quantities of two neutron transfer (p,t) reactions. In order to simplify the development of our (p,t) model and begin with relatively simple cases, we make the following assumptions:

- The target nucleus under consideration is even-even, i.e. it possesses even numbers of both protons and neutrons, is spherical, and in its ground state has a spin and parity assignment of $J^\pi = 0^+$.
- The two neutrons are transferred simultaneously, in one step, as a single *di-neutron* object.

In later sections we will explore the validity of these assumptions and also describe the requirements for incorporating additional physics into our model.

2.1 The Nuclear Shell Model

The nuclear shell model shares many analogies with the atomic shell model. As in the case of electrons, nucleons sequentially fill discrete orbits around a central potential. The filling of these orbits, or shell model states, follows simple rules, in particular the Pauli exclusion principle. The exclusion principle states that two

fermions (particles with an intrinsic spin of $s = 1/2$ such as neutrons and protons) cannot occupy the same space whilst having the same set of *quantum numbers*.

The quantum numbers of the shell model are n, l, s, j and m. The principal quantum number n is related to the number of radial nodes in a nucleon's wavefunction, l is the orbital angular momentum, s the intrinsic spin angular momentum, and j the total angular momentum of the nucleon. m is the magnetic substate of the nucleon which is the projection of j onto an arbitrary z-axis.

Protons and neutrons occupy the shell model orbitals independently of each other as the two particle types differ by an additional quantum number, referred to as isospin projection t. The maximum occupancy of an orbital is equal to $2(2l+1)$.

Quantum number	Values
n	$n = 0, 1, 2, \ldots$
l	$l = 0, 1, 2, \ldots$
s	$s = \pm 1/2$
j	$j = l \pm s$
m	$-j \leq m \leq +j$

Table 2.1: The rules governing the allowed values of the shell model quantum numbers.

In the atomic shell model case, the central potential is due to the electromagnetic force ~~emanating~~ from the positively charged nucleus. However, in the nuclear shell model the potential is instead an average potential generated by the strong nuclear force of the other nucleons present in the nucleus. In the development of the nuclear shell model a number of different models for the potential were explored. Nucleons which populate states in the same nucleus, but with differing quantum numbers, will have wavefunctions of differing energies. The greater the energy of a nucleon's orbit, the smaller its binding energy in the nucleus. It is found that there are significant energy gaps between groups of orbitals. Groupings of orbitals between energy gaps are referred to as *shells*.

These shells correspond to physical observables in the chart of the nuclides. It is found that nuclei with numbers of protons and neutrons which correspond to

complete fillings of shells are more stable than nuclei with only partially filled shells. The numbers of protons and neutrons which correspond to filled shells are referred to as *magic* numbers. These magic numbers are found empirically to be: 2, 8, 20, 28, 50, 82, 126 with 40 also sometimes referred to as *semi*-magic [].

The potential used for calculations of the shell model orbitals must reproduce these magic numbers (along with other observed quantities). The simplest potential to apply is that of a square well, where the nucleons experience a potential $V(r)$ described by

$$V(r) = -V_0 \quad r \leq R$$
$$V(r) = 0 \quad r > R\,. \tag{2.1}$$

This square well however is an obvious oversimplification and also does not reproduce the expected magic numbers []. The harmonic oscillator is another simple class of potential which may be applied. It has the form of

$$V(r) = \frac{1}{2}m\omega^2 r^2\,, \tag{2.2}$$

where m is the mass of the nucleon, r its radial distance and ω the angular frequency of the oscillator []. Solutions for nucleon wavefunctions orbiting within an oscillator potential perform much better than those of the square well. However, the calculated magic numbers, or shell closures, do not match the physical data above $N, Z = 40$. In addition, many orbitals are now degenerate in energy with one another which was not the case for the square well potential.

The next potential applied is often referred to as a *Woods-Saxon* potential and is an extension of the harmonic oscillator case, but with the bottom of the well smoothed out via the introduction of an attractive l^2 term []. This smoothing of the bottom of the well serves to lift the degeneracy of the calculated levels. The form of the Woods-Saxon potential is

$$V(r) = \frac{-V_0}{1 + e^{\frac{r-R}{a}}}\,, \tag{2.3}$$

where a is the *skin-thickness* of the potential, or the radial distance over which the potential falls from 90% strength to 10%. Unfortunately, levels calculated using this potential form do not completely match the experimentally measured shell gaps and occupancies. An additional *spin-orbit* term is therefore added to the Woods-Saxon potential. This spin-orbit term is a predominately surface effect and has the form

$$V_{l.s} = -V_{ls}\frac{\partial V(r)}{\partial r} l.s \,, \tag{2.4}$$

where $V(r)$ is a Wood-Saxon potential and V_{ls} is the strength of the spin-orbit interaction. The $l.s$ factor is dependent upon how l and s couple to form the total angular momentum j of the nucleon. $l.s$ is given by

$$l.s = \frac{1}{2}\left(j^2 - l^2 - s^2\right) \tag{2.5}$$

and so its value will differ depending upon whether $j = l + s$ or $j = l - s$. The energy levels of states calculated using a potential which includes this spin-orbit term will therefore depend on j and so single orbitals predicted previously are now split in energy. The maximum occupancy of each of these split levels is equal to $2j + 1$. Figure 2.1 gives the shell model level structure and occupancies predicted by this final potential.

States are labelled according to their values of n, l and j, with the l values usually given by their historical spectroscopic letter notations. Table ?? gives the corresonding letter for each value of l.

l letter	s	p	d	f	g	h	i
l value	0	1	2	3	4	5	6

Table 2.2: Spectroscopic notation for different values of l.

These shell model levels and associated quantum numbers are considered to be a good representation of reality for spherical nuclei, close to the line of nuclear stability. For deformed or very unstable nuclei the validity of the shell model begins

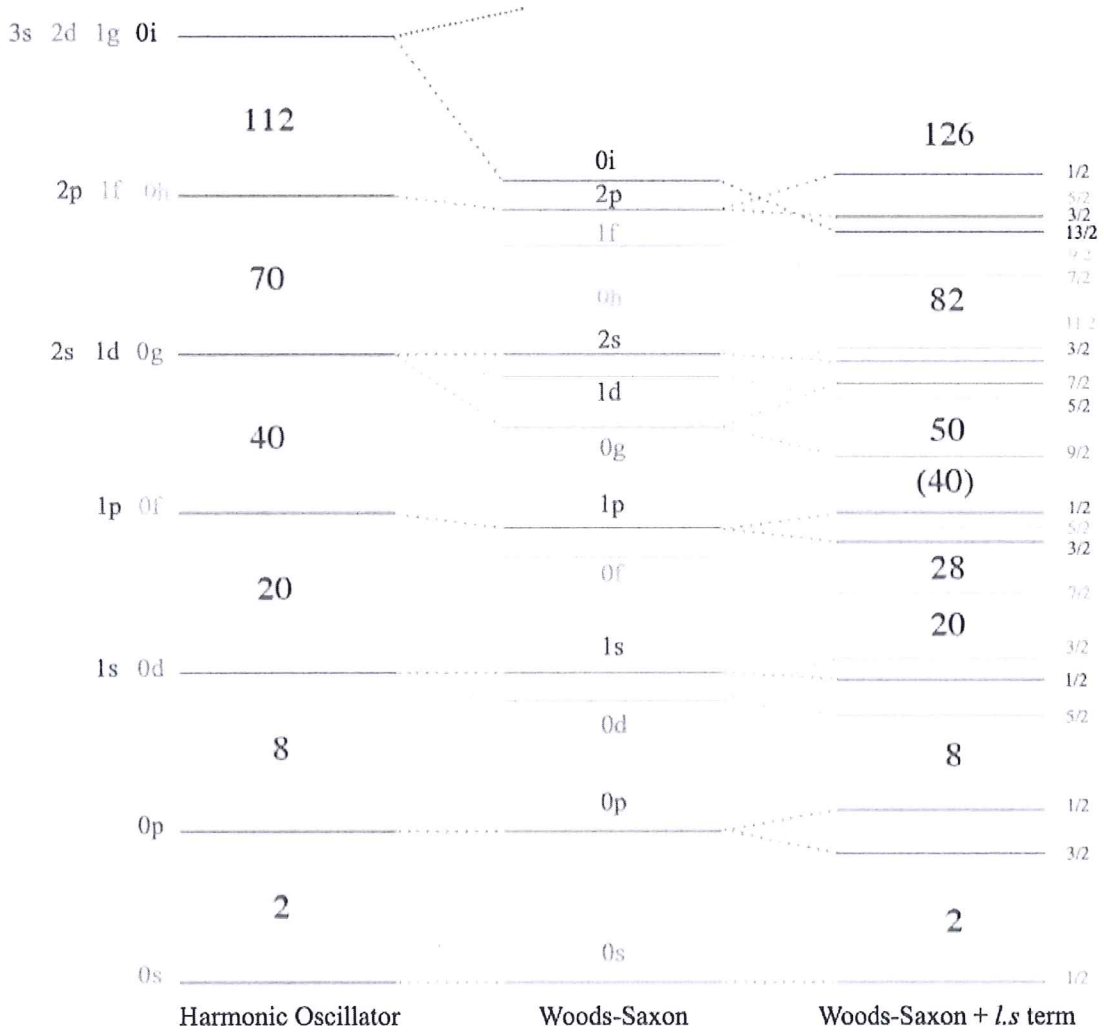

Figure 2.1: Shell model states and shell occupancies predicted using different forms for the central potential. Figure taken and adapted from [].

S. particle

mean field

to break down and new levels schemes and *good* quantum numbers are required []. If our model is applied to non-spherical nuclei, we must take these differences into account.

2.1.1 Optical Model Potentials

A relatively simple compound nucleus reaction model is that of the *optical model*. In this model a wavefunction representing a nucleon incident on a nucleus experiences a mean field potential due to the other nucleons present and experiences scattering similar to that of light incident on a partially opaque sphere. This potential includes both real and imaginary terms,

$$V(r) = U(r) + iW(r)\,.$$

The imaginary term simulates an absorption of particles into the compound nucleus formed in the reaction. In other words, the potential is *not* conservative.

In this study we are not concerned with calculating compound nucleus reactions, but in the Distorted Wave Born Approximation, to be described, the effect of competing compound nucleus reaction channels is taken into account via an optical model potential.

The real term of the potential, $U(r)$, is generally a sum of a Wood-Saxon *volume* potential, a spin-orbit term, and, if the incident particle is charged, an additional Coulomb term. The imaginary potential generally consists of a Wood-Saxon volume potential and a surface term of the form []

$$W_{\mathrm{s}}(r) = \frac{\partial W_V(r)}{\partial r}\,. \qquad (2.6)$$

2.2 Spectroscopy

The single particle states of a nucleus, as understood in terms of the shell model, may be experimentally investigated via the use of single particle transfer reactions,

e.g. (p,d) or (d,p), ~~in a process~~ referred to as *spectroscopy* []. The short reaction timescales of direct transfer reactions, combined with the interaction of the incident particle with only one, or possibly two, nucleons in the target nucleus, allows for the excitation of ~~single~~ particle, or hole, states in the residual nucleus. The ~~single~~ particle, or hole, states can be assumed to be that of pure ~~shell~~ model states [].

The orbital angular momentum l of the excited state, or hole, can be determined by an analysis of the angular distribution of the outgoing light particle, as this is determined by the angular momentum transferred by the stripped, or picked up, ~~single particle~~. The analysis of direct transfer reactions is usually carried out via the Distorted Wave Born Approximation (DWBA) method. In an example case: a target $A+1$ body nucleus is bombarded by a beam of protons which pickup neutrons from the valence orbitals (or more deeply bound orbitals if the proton energy is high enough) via the (p,d) reaction. The angular distribution of the outgoing deuterons, within a small energy range, is measured and matched against DWBA calculations to determine from which ~~shell model~~ orbital the neutron has been taken. The residual nucleus is left in an excited state, due to the hole created, and will subsequently decay, generally via the emission of γ-rays. The decay of this excited hole state can be measured and the energy of an excited state of the residual A body nucleus can be determined.

So, via the study of the energies and angular distributions of these excited states, it is possible to buildup a complete picture of the excited level structure of the residual nucleus.

Two nucleon transfer reactions can also be studied using the same framework. The study of these reactions is typically performed to investigate the strength of the correlations and pairings between the single particle ~~shell~~ model states in a target nucleus []. However, two nucleon transfers may also be used to study the excited level structure of a nucleus, especially states which may only be weakly populated via single particle transfer reactions.

2.3 The Distorted Wave Born Approximation

2.3.1 The Plane Wave Born Approximation

The quantities of interest to be calculated for a transfer reaction are the angle-integrated cross section σ_{tot} and the differential cross section $\frac{d\sigma}{d\Omega}(\theta)$ for populating a specific final state. Due to the kinematics of a transfer reaction, the differential cross section, that determines the angular distribution of the light-particle following the collision, will depend upon which state of the target nucleus has been populated. Therefore, this allows theoretically calculated angular distributions to be used to determine which state has been populated in an experiment via the angular distribution of the measured fragments.

By considering a simplified model of single particle transfer, in which the wave-functions of the projectile in the incident and outgoing stages are assumed to have the form of plane waves, we may qualitatively derive this relation between the differential cross section and the state of the target nucleus which becomes populated.

The differential cross section for the transition from a state α to a state β is related to the T matrix element $T_{\beta,\alpha}$ by,

$$\frac{d\sigma}{d\Omega} = G|T_{\beta,\alpha}|^2 \ , \tag{2.6}$$

where G is a term containing various phase space parameters. These are unnecessary for the present qualitative discussion.

Before performing any transfer calculations, it is beneficial to gain a clear understanding of the co-ordinate system to be used. The co-ordinate system for a single particle transfer, (p,d) or (d,p), reaction is given below in figure 2.2. The coordinates of the proton and the deuteron may be seen from figure 2.2 to be given by,

$$\vec{r}_p = \frac{A}{A+1}\vec{r}_n - \vec{r} \ , \tag{2.7}$$

$$\vec{r}_d = \vec{r}_n - \frac{\vec{r}}{2} \ , \tag{2.8}$$

where A is the mass number of the target nucleus in the (d,p) case. The factor of $\frac{A}{A+1}$ will appear frequently in the coming sections and as such will be referred to as μ in order to simplify the various expressions derived.

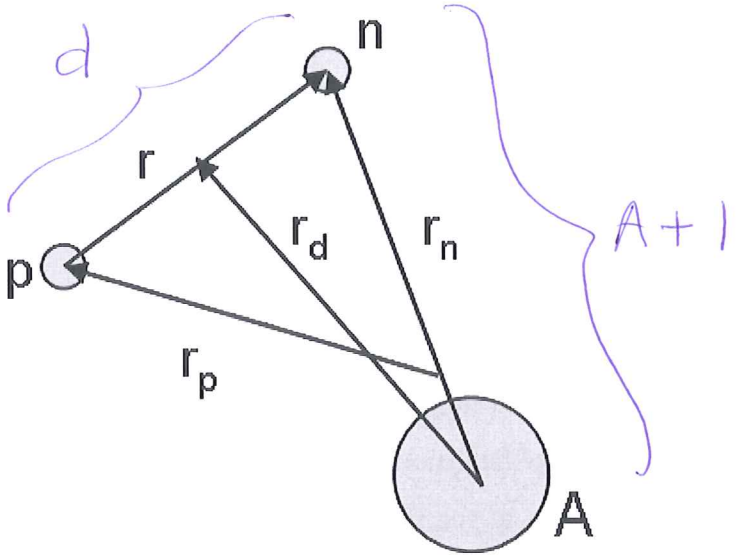

Figure 2.2: A+1(p,d)A or A(d,p)A+1 single particle transfer coordinate system.

The Born Approximation[?] (referred to in the rest of this work as the Plane Wave Born Approximation (PWBA), in order to distinguish it from the Distorted Wave Born Approximation) gives the T matrix element, in Dirac's bra(c)ket notation, as,

$$T_{\beta,\alpha} = \langle \vec{k}_\beta \Phi_\beta | V_{\alpha\beta} | \vec{k}_\alpha \Phi_\alpha \rangle \ ,$$

where $V_{\alpha\beta}$ is the potential coupling state α to state β, k_α and k_β are the wavenumbers of the incident and outgoing waves respectively, and Φ_α and Φ_β are the wavefunctions of the target nucleus in the channels α and β respectively.

In the PWBA, we assume the relative motion of the projectile and target nuclei in the initial and final states are extremely simplified versions of the actual physical system. For simplicity we will also ignore the presence of intrinsic spin during the following discussion. Here, we shall assume a (d,p) reaction, but the same results hold for other transfer reactions.

The initial state is that of a plane wave describing the motion of the incident

I feel this is a chance to start describing some angular momentum etc. It is very schematic and a wasted opportunity.

deuteron, multiplied by ~~a term describing~~ the internal wavefunction of the deuteron, and ~~a term describing~~ the nuclear wavefunction of the mass A target nucleus. The final state is ~~a combination of~~ a plane wave describing the motion of the outgoing proton ~~and a term describing~~ the nuclear wavefunction of the final mass A+1 nucleus. So, this includes a wavefunction describing the behaviour of the transferred neutron which is assumed to now be bound in a single particle wavefuntion in the target nucleus. Our initial and final states are therefore,

and the proton spin?

?

Could have written T_{fi} before?

notation changed? now $|i\rangle$, $|f\rangle$ before $T_{\beta,\alpha}$.

$$|i\rangle = \left|\vec{k}_d, \phi_d \Phi(A)\right\rangle$$

and

no spin labels no α, β?

$$|f\rangle = \left|\vec{k}_p, \Phi(A+1)\right\rangle .$$

Assume single particle model in which Φ_A etc slater det?

If we assume that the A nucleons which make up the target nucleus occupy only closed shells, i.e. that the nucleus is magic, and that the transferred neutron is deposited into the next available ~~shell model~~ s. part orbital, we may simplify the overlap of the A and $A+1$ nuclear wavefunctions;

ang. momentum?

$\langle \Phi(A+1)|\Phi(A)\rangle \approx \phi^*(\vec{r}_n)$, means?

$1/\sqrt{N}$ if N neutrons (identical particles)

← where ϕ_n is the wavefunction of the transferred nucleon bound to the A nucleon core. $\langle\ |\ \rangle$ is integrated over A nucleons. This simplification allows the initial and final states to be written as,

coordinates

$$|i\rangle = |\vec{k}_d, \phi_d\rangle \equiv e^{i\vec{k}_d \cdot \vec{r}_d} \phi_d(\vec{r})$$

and,

no spin labels

$$|f\rangle = |\vec{k}_p, \phi_n\rangle \equiv e^{i\vec{k}_p \cdot \vec{r}_p} \phi_n(\vec{r}_n) .$$

Transfer reactions are generally found to occur near the surface of the target nucleus and involve only one interaction. The potential coupling the initial and final states may be approximated as due to the potential between the proton and neutron comprising the deuteron $V_{n,p}(\vec{r})$. [refs]

not n,p later but np

When the bracket notation is written in integral form, the expression for $T_{\beta,\alpha}$ is now,

$$T_{p,d} = \int e^{-i\vec{k}_p\cdot\vec{r}_p}\phi_n^*(\vec{r}_n)V_{n,p}(\vec{r})\phi_d(\vec{r})e^{i\vec{k}_d\cdot\vec{r}_d}d\vec{r}_d d\vec{r} \ . \tag{2.9}$$

We may reduce the number of different coordinates over which to integrate, by first rewriting $e^{i\vec{k}_p\cdot\vec{r}_p}$ and $e^{i\vec{k}_d\cdot\vec{r}_d}$ in terms of the coordinates of the transferred neutron by recalling expressions (2.7) and (2.8);

$$e^{i\vec{k}_d\cdot\vec{r}_d}e^{-i\vec{k}_p\cdot\vec{r}_p} = e^{i\vec{k}_d\cdot\vec{r}_d - i\vec{k}_p\cdot\vec{r}_p} = e^{i\vec{r}_n(\vec{k}_d-\vec{k}_p\mu)+i\vec{r}(\vec{k}_p-\frac{\vec{k}_d}{2})} = e^{i\vec{k}_n\cdot\vec{r}_n}e^{i\vec{Q}\cdot\vec{r}} \ . \tag{2.10}$$

We may then introduce $\vec{k}_n$ and $\vec{Q}$ which are, respectively, the 'wavenumber' of the neutron and a wavenumber related to the relative motion of the neutron and proton;

$$\vec{k}_n = \vec{k}_d - \vec{k}_p\mu \ ,$$

$$\vec{Q} = \vec{k}_p - \frac{\vec{k}_d}{2} \ .$$

Following the introduction of $\vec{k}_n$ and $\vec{Q}$, the integral for T thus becomes the product,

$$T_{p,d} = \int d\vec{r}_n\{\phi_n^*(\vec{r}_n)e^{i\vec{k}_n\cdot\vec{r}_n}\}\int d\vec{r}\{e^{i\vec{Q}\cdot\vec{r}}V_{np}(\vec{r})\phi_d(\vec{r})\} \ . \tag{2.11}$$

We have changed the basis of integration from $\vec{r}_d$ to $\vec{r}_n$, however the Jacobian determinant for this change will be unity, as may be seen from expression (2.7). For the case of our qualitative discussion here, we introduce a zero range approximation for the potential $V_{np}(\vec{r})$, i.e. we assume that $V_{np}(\vec{r})\phi_d(\vec{r})$ is a short range object and that the potential acts over approximately zero range, $\vec{r} \approx 0$. We make the replacement $V_{np}(\vec{r})\phi_d(\vec{r}) \approx D_0\delta(r)$ where D_0 is a constant equal to the volume integral of the potential and the internal deuteron wavefunction.

In the zero range limit,

$$D_0 = \int V_{np}(\vec{r})\phi_d(\vec{r})d\vec{r}$$

and hence

$$\int \{e^{i\vec{Q}\cdot\vec{r}} V_{np}(\vec{r})\phi_d(\vec{r})\}d\vec{r} \approx e^{i\vec{Q}\cdot 0} D_0 = D_0 \ . \tag{2.12}$$

For a (d,p) or (p,d) reaction, D_0 is typically assumed to have a value of -122.5 MeV fm$^{3/2}$ [?].

Our expression for T is now,

$$T_{p,d} \propto D_0 \int \{\phi_n^*(\vec{r}_n) e^{i\vec{k}_n\cdot\vec{r}_n}\}d\vec{r}_n \ . \tag{2.13}$$

Thus, $\vec{k}_n$ represents the linear momentum transfer between the initial and final states $\vec{k}_n = \vec{k}_d - \vec{k}_p\mu$, which will depend upon the angle between $\vec{k}_d$ and $\vec{k}_p$. It may be seen from (2.13) that the value of T (and hence $\frac{d\sigma}{d\Omega}$) for each angle between $\vec{k}_d$ and $\vec{k}_p$ is simply related to the Fourier transform of the bound neutron's wavefunction. Therefore, the observed angular distribution of the outgoing projectile may be used to determine which state of the nucleus the transferred particle has been deposited into or removed from. These features are expected to persist in the presence of distorting interactions between the projectile(s) and target.

2.3.2 Distorted waves

The PWBA method treats the transfer reaction as a weak interaction (perturbation) to the incident wavefunction and is therefore only valid when the optical model potential (OMP) is ignored.

The Distorted Wave Born Approximation (DWBA) extends the approach of the PWBA by replacing the ingoing and outgoing plane waves with *distorted* waves; solutions to the Schrödinger equation in which the particles are scattered by an OMP appropriate for the target nucleus. This has the effect of taking into account the non-elastic and elastic scattering reactions which the incident particles implicitly undergo,

In calculations of nucleon-nucleus collisions, a mean-field complex optical potential is used to simulate the complicated many-body interaction which the nucleon would experience due to the A nucleons of the nucleus. The real part of this potential simulates the elastic scattering of the incident nucleons due to the nuclear potential well. The imaginary component simulates the absorption of incoming nucleons into non-elastic channels, which include all reactions which occur via a compound nucleus.

The T matrix element for the transfer reaction from channel α to β is now given by,

$$T_{\beta,\alpha} = \langle \chi_\beta^{(-)} \Phi_\beta | V_{\alpha\beta} | \Phi_\alpha \chi_\alpha^{(+)} \rangle \ . \tag{2.14}$$

Here the χ^- and χ^+ are ingoing and outgoing distorted waves, respectively, and $\Phi_{\alpha,\beta}$ are the nuclear wavefunctions of the target nucleus in each channel.

The use of the standard DWBA method continues to assume that the reaction takes place in a single step (Born Approximation), with the transferred nucleon (or cluster) being added to/removed from a specific shell model state.

2.3.3 Two neutron DWBA

Here we extend the methods developed above to derive the two particle transfer DWBA formalism, for the case of the (p,t) reaction for a 0^+ spin, $A+2$ mass target nucleus.

The differential cross section for a specific J transfer is given by (2.15). In an experiment, the incident beam of particles will typically be unpolarised and the orientation of the spin of the target nucleus will also be unknown, as will the spin projections of the final particles (without measurement). Therefore, the cross section includes a summation of transitions over all of the final possible projections, and an average over all the possible spin projections of the initial state [?];

$$\frac{d\sigma}{d\Omega}(0^+ \to J^\pi) = G \frac{1}{(2S_p+1)} \sum_{\sigma_p \sigma_t M} |T_{JM\sigma_t,\sigma_p}|^2 \tag{2.15}$$

The coordinate system for (p,t) or (t,p) two neutron transfer is illustrated in

figure 2.3. As can be seen, the position vectors for the proton and triton are;

$$\vec{r}_t = \vec{r}_n - \frac{\vec{\rho}}{3} , \tag{2.16}$$

$$\vec{r}_p = \frac{A}{A+2}\vec{r}_n - \vec{\rho} . \tag{2.17}$$

For simplicity, from this point onwards, we will replace $\frac{A}{A+2}$ with μ.

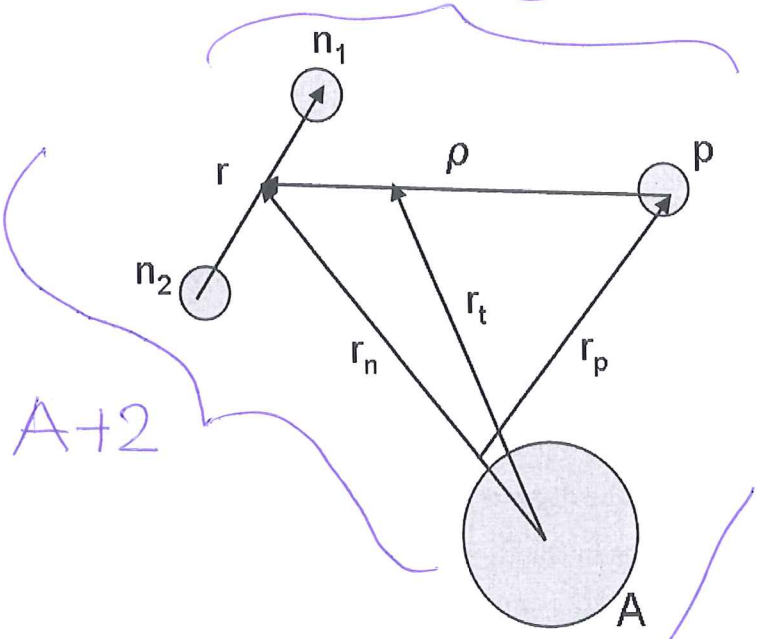

Figure 2.3: (p,t) or (t,p) two neutron transfer coordinate system.

The initial and final states of the (p,t) system are;

$$|i\rangle = |\Phi(A+2)_{0^+}\chi_{\vec{k}_p}\chi_{p\sigma_p}\rangle \tag{2.18}$$

and,

$$|f\rangle = |\Phi(A)_{JM}\chi_{\vec{k}_t}\phi_{t\sigma_t}\rangle \tag{2.19}$$

where $\chi_{\vec{k}_p}$ and $\chi_{\vec{k}_t}$ are distorted wavefunctions for the proton and triton respectively, describing elastic scattering from appropriate OMPs. For simplicity it will be assumed that the OMPs for this example contain no spin-orbit terms. $\phi_{t\sigma_t}(\vec{\rho},\vec{r})$ is the internal wavefunction of the triton (including a component accounting for its

intrinsic spin), $\chi_{p\sigma_p}$ is an intrinsic spin wavefunction of the proton, and $\Phi(A+2)_{0^+}$ and $\Phi(A)_{JM}$ are the internal wavefunctions of the target nucleus before and after the transfer respectively.

The internal triton wavefunction $\phi_{t\sigma_t}(\vec{\rho},\vec{r})$ will be decomposed into a product of a 0^+ di-neutron wavefunction $\phi_{2n}(\vec{r})$, a wavefunction representing the motion of the proton relative to the di-neutron (assumed to be s state) $f(\vec{\rho})$, and a triton (proton) spin wavefunction $\chi_{p\sigma_t}$;

$$\phi_{t\sigma_t}(\vec{\rho},\vec{r}) = \phi_{2n}(\vec{r})f(\vec{\rho})\chi_{p\sigma_t} \ . \tag{2.20}$$

The overlap integral of the wavefunctions of the nucleus in its initial and final states, $\langle\Phi(A)_{JM}|\Phi(A{+}2)_{0^+}\rangle$, may be simplified by assuming that a core of A nucleons is unchanged following the removal of the 2 neutrons from the $A+2$ initial state. We start by assuming that the wavefunction of the initial $A+2$ nucleus may be decomposed into a product of the wavefunction for the A nucleon core $\Phi(A)_{JM}$, a bound state wavefunction for the di-neutron $\phi^{2n}_{NL\Lambda}(\vec{r}_n)$ and a wavefunction describing the motion of the two neutrons in the di-neutron relative to one another $\phi_{2n}(\vec{r})$. The product of these two wavefunctions will be weighted by a Clebsh-Gordon coefficient, which is determined by the angular momenta of the two states.

The bound di-neutron has 0^+ intrinsic spin, an orbital angular momentum L and an orbital angular momentum projection Λ. The intrinsic spin J and spin projection M of the A nucleon core couple with the L and Λ of the bound di-neutron to give a total angular momentum of 0^+ for the initial $A+2$ nucleus.

The coupling of these angular momenta states is illustrated in figure 2.4.

$$\Phi(A+2)_{0^+} = \sum_{M\Lambda}(JML\Lambda|00)\phi^{2n}_{NL\Lambda}(\vec{r}_n)\phi_{2n}(\vec{r})\Phi(A)_{JM} \tag{2.21}$$

Systems which couple to $|00\rangle$ states are a special case and may be simplified, e.g.

$$(j_1m_1j_2m_2|00) = \delta_{j_1j_2}\delta_{m_1-m_2}\frac{(-1)^{j_1-m_1}}{(2j_2+1)^{1/2}} \ . \tag{2.22}$$

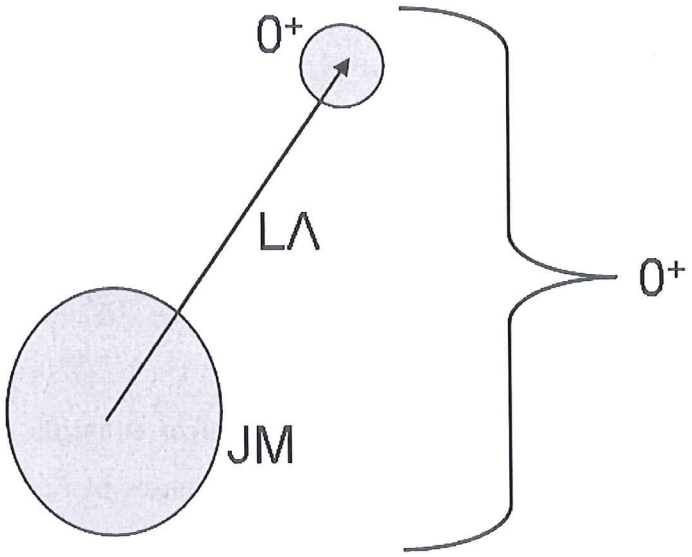

Figure 2.4: Illustration of the various angular momentum states which are coupled together in the A+2 system.

Our expression for coupling to $|00\rangle$ therefore becomes,

$$\Phi_{0^+}(A+2) = \sum_{M\Lambda} \frac{(-)^{J-M}}{(2J+1)^{1/2}} \delta_{JL}\delta_{M-\Lambda}\phi^{2n}_{NL\Lambda}(\vec{r}_n)\phi_{2n}(\vec{r})\Phi_{JM}(A) \ . \tag{2.23}$$

The overlap integral between initial and final states is therefore;

$$\langle \Phi_{A_{JM}} | \Phi_{(A+2)_{0^+}} \rangle = \frac{(-)^{J+\Lambda}}{(2J+1)^{1/2}} \phi^{2n}_{NJ\Lambda}(\vec{r}_n)\phi_{2n}(\vec{r}) \ . \tag{2.24}$$

We may also see that our sum over the proton and triton spins is trivially given by;

$$\sum_{\sigma_p\sigma_t} \chi_{p\sigma_t}\chi_{p\sigma_p} = \delta_{\sigma_p\sigma_t} \ . \tag{2.25}$$

The expression for T is now given by,

$$T = \frac{(-)^{J+\Lambda}}{(2J+1)^{1/2}} \int \Psi^*_{\vec{k}_t,\vec{r}_t} \Psi_{\vec{k}_p,\vec{r}_p} \phi^*_{2n}(\vec{r})\phi_{2n}(\vec{r})V_{p2n}(\vec{\rho}) f^*(\vec{\rho})\phi^{2n}_{NJ\Lambda}(\vec{r}_n) d\vec{r}_t d\vec{\rho} d\vec{r} \ . \tag{2.26}$$

$\int \phi^*_{2n}(\vec{r})\phi_{2n}(\vec{r})d\vec{r} = 1$ and so we may reduce the number of dimensions over which to integrate;

$$T = \frac{(-)^{J+\Lambda}}{(2J+1)^{1/2}} \int \Psi^*_{\vec{k}_t,\vec{r}_t} \Psi_{\vec{k}_p,\vec{r}_p} V_{p2n}(\vec{\rho}) f^*(\vec{\rho}) \phi^{2n}_{NJ\Lambda}(\vec{r}_n) d\vec{r}_t d\vec{\rho} \ . \tag{2.27}$$

The bound state wavefunction of the di-neutron may be separated into radial and angular components;

$$\phi^{2n}_{NJ\Lambda}(\vec{r}_n) = \frac{U_{NJ}(r_n)}{r_n} Y^{\Lambda}_J(\hat{r}_n) \ , \tag{2.28}$$

where $U_{NJ}(r_n)$ is a solution of the radial Schrödinger equation and $Y^{\Lambda}_J(\hat{r}_n)$ is a spherical harmonic, a function of the angular coordinates of $\vec{r}_n$ (i.e. $Y^{\Lambda}_J(\hat{r}_n) = Y^{\Lambda}_J(\theta,\phi)$).

As was the case in section 2.3.1, the calculation of T will be simplified if we assume that $V_{p2n}(\vec{\rho}) f^*(\vec{\rho})$ is a zero range object; $V_{p2n}(\vec{\rho}) f^*(\vec{\rho}) \propto \delta(\vec{\rho})$. We may again introduce a constant D_0 which represents the strength of the zero range vertex;

$$\int V_{p2n}(\vec{\rho}) f^*(\vec{\rho}) d\vec{\rho} = D_0 \ . \tag{2.29}$$

For a (p,t) or (t,p) reaction, D_0, typically, has a value of -469 MeV fm$^{3/2}$ [?].

Using the zero range approximation, the integral for T becomes,

$$T = D_0 \frac{(-)^{J+\Lambda}}{(2J+1)^{1/2}} \int \Psi^*_{\vec{k}_t,\vec{r}_t} \Psi_{\vec{k}_p,\vec{r}_p} \phi^{2n}_{NJ\Lambda}(\vec{r}_n) d\vec{r}_t \ . \tag{2.30}$$

It is now convenient to again move from a DWBA to a PWBA description as this will allow the physics of the problem to be more readily understood. The distorted waves for the proton and triton are replaced with plane waves independent of any OMP;

$$\Psi_{\vec{k}_p,\vec{r}_p} \rightarrow \psi(\vec{k}_p,\vec{r}_p) = e^{i\vec{k}_p\cdot\vec{r}_p} \ , \tag{2.31}$$

$$\Psi^*_{\vec{k}_t,\vec{r}_t} \rightarrow \psi^*(\vec{k}_t,\vec{r}_t) = e^{-i\vec{k}_t\cdot\vec{r}_t} \ . \tag{2.32}$$

In the zero range limit we may rewrite the product of these two plane waves as